Vibronic structure of the NO_3 $\tilde{X}\ ^2A_2'$ system

Masaru Fukushima

Graduate School of Information Sciences, Hiroshima City University,
Hiroshima 731-3194, Japan

Background

1985 Kawaguchi et al. — IR spectroscopy

Assigned 1492 cm^{-1} band to be the ν_3 fundamental

2007 Stanton — ab initio calculation

Asserted 1492 cm^{-1} band should be $\nu_3+\nu_4$, and ν_3 should be ~ 1000 cm^{-1}

2008 Jacox and Thompson — Matrix isolation spectroscopy

Observed several isotopomers

2011 Kawaguchi et al. — IR spectroscopy

Observed and assigned $\nu_3 + \nu_4 - \nu_4$ hot band, and confirmed the $\nu_3+\nu_4$ assignment

2013 Fukushima and Ishiwata — Dispersed fluorescence spectroscopy

Observed jet cooled spectra of $^{14}NO_3$ and $^{15}NO_3$, and found a new band in the ν_1 fundamental region, ~ 1050 cm^{-1}, and the ν_1 isotope shift indicates it is assigned to be an a_1' band (3 ν_4)

2016 Fukushima and Ishiwata — 2C-R4WM spectroscopy

Rotationally resolved spectra at the ν_1 fundamental and traditional ν_3 fundamental regions

Experiment

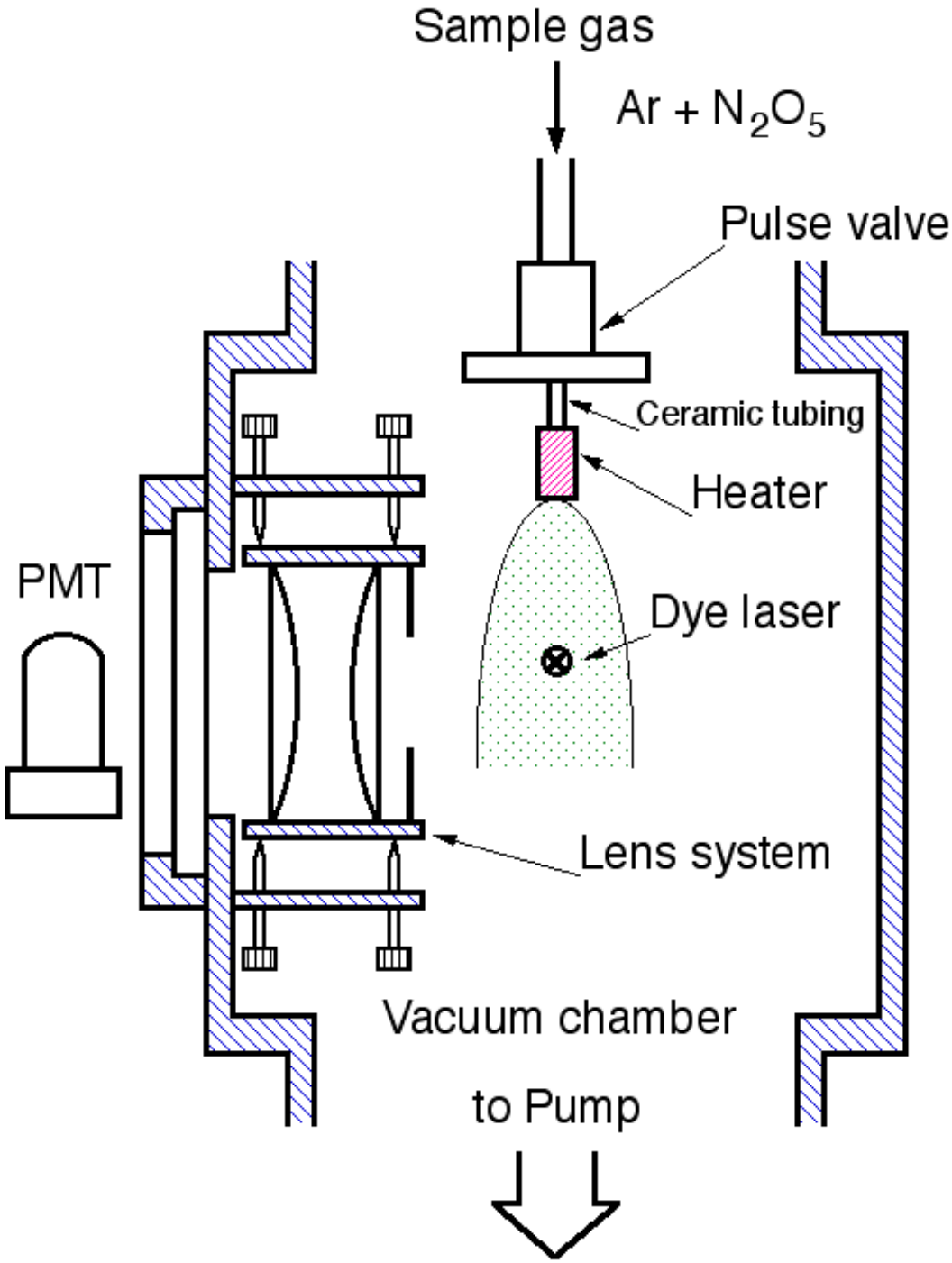
Sample gas
Ar + N_2O_5
Pulse valve
Ceramic tubing
Heater
PMT
Dye laser
Lens system
Vacuum chamber
to Pump

0+0 cm^{-1} band excitation

$\tilde{B}\ ^2E' - \tilde{X}\ ^2A_2'$

$^{14}NO_3$

resolution : ~ 10 cm^{-1} (fwhm)
(monochromator settings)

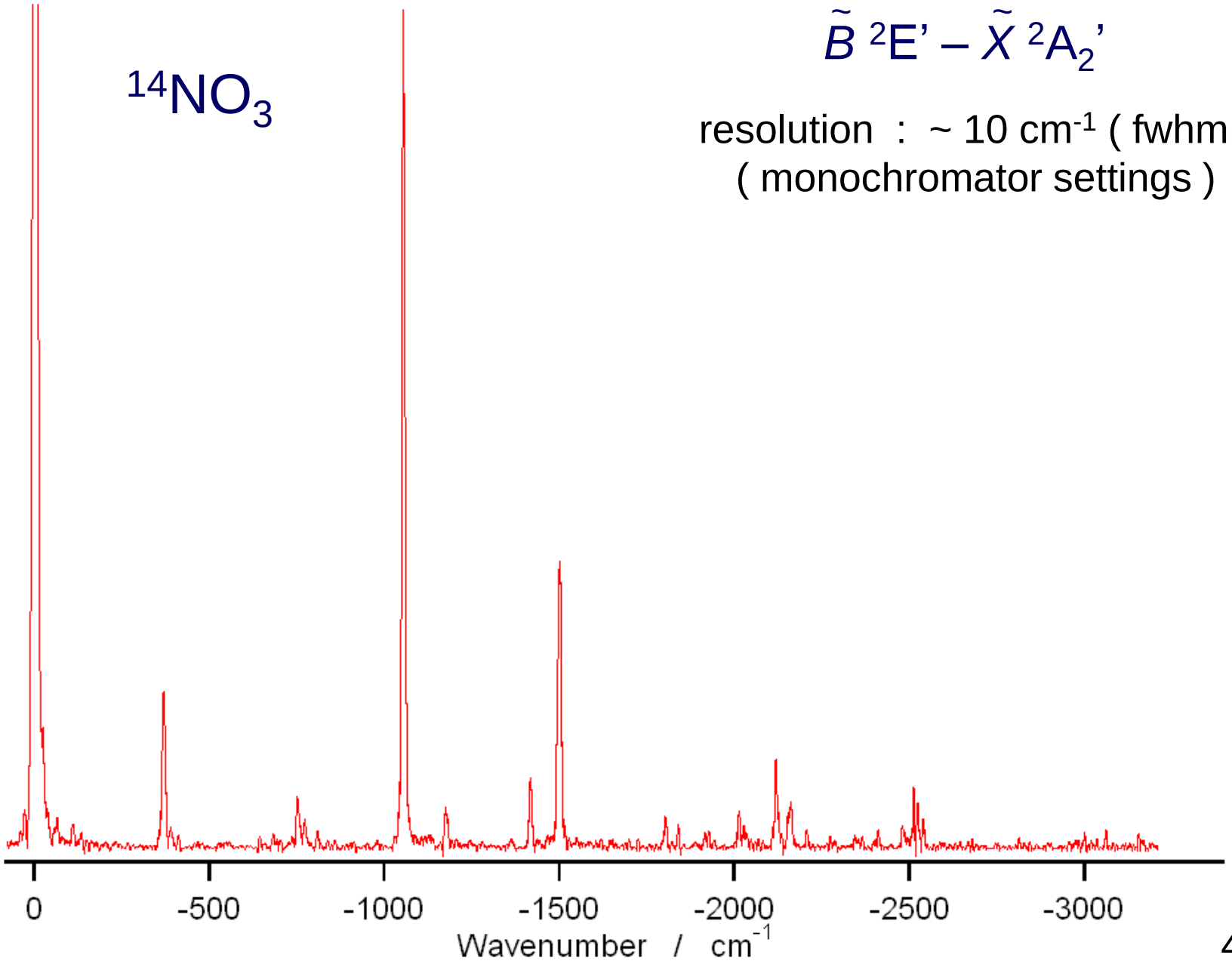

0+0 cm^{-1} band excitation

$\tilde{B}\ ^2E' - \tilde{X}\ ^2A_2'$

resolution : ~ 10 cm^{-1} (fwhm)
(monochromator settings)

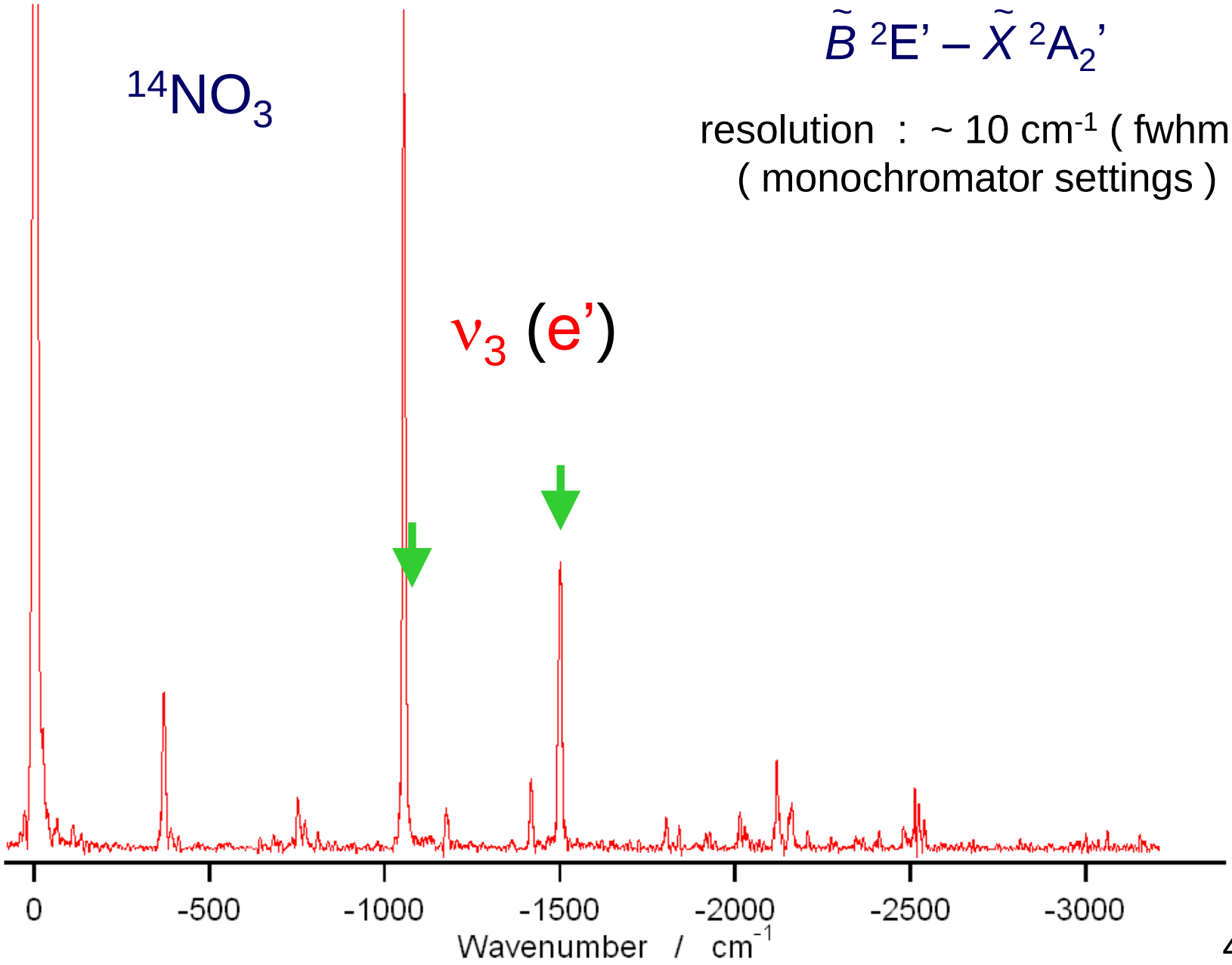

0+0 cm^{-1} band excitation

$\tilde{B}\ ^2E' - \tilde{X}\ ^2A_2'$

resolution : ~ 10 cm^{-1} (fwhm)
(monochromator settings)

$^{14}NO_3$

ν_3 (e')

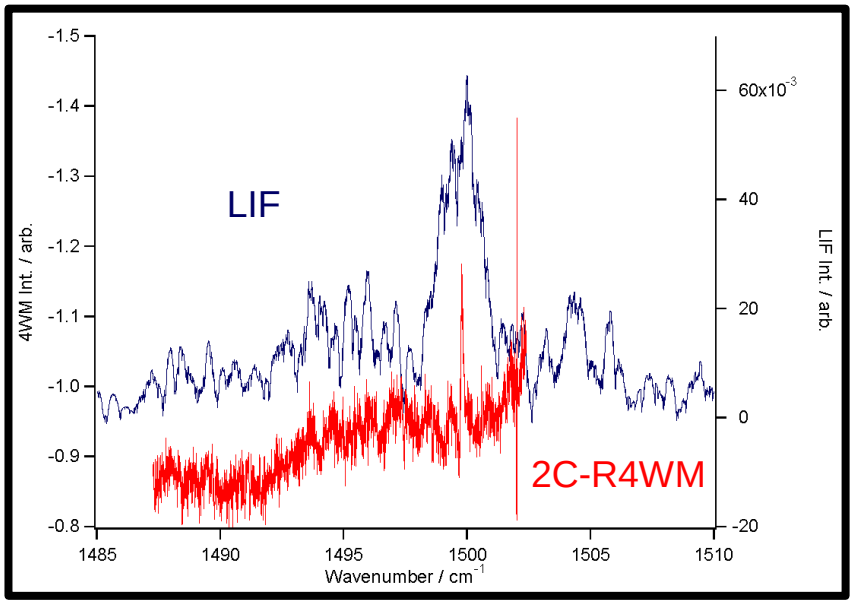

0 -500 -1000 -1500 -2000 -2500 -3000

Wavenumber / cm^{-1}

0+0 cm^{-1} band excitation

$\tilde{B}\ ^2E' - \tilde{X}\ ^2A_2'$

resolution : ~ 10 cm^{-1} (fwhm)
(monochromator settings)

$^{14}NO_3$

ν_3 (e')

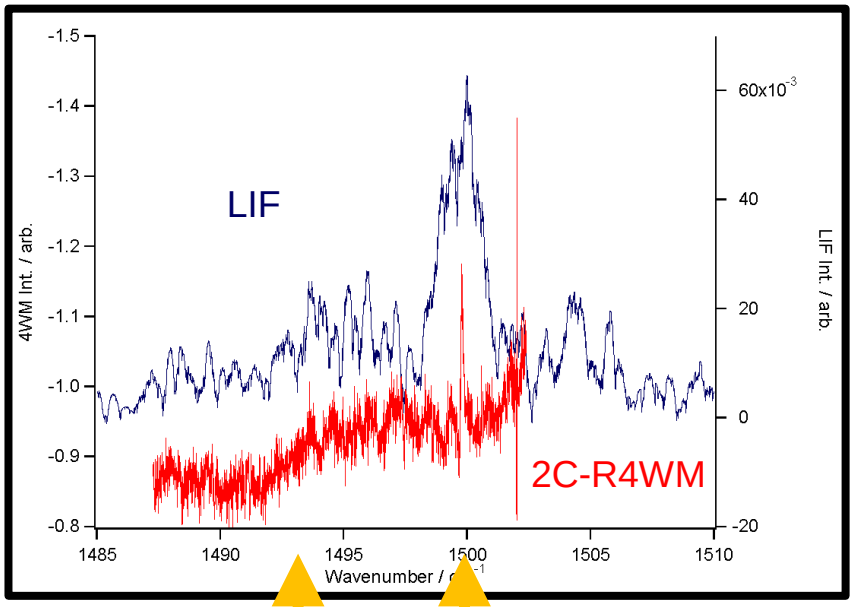

e' a_1'

0 -500 -1000 -1500 -2000 -2500 -3000
Wavenumber / cm^{-1}

0+0 cm^{-1} band excitation

$\tilde{B}\ ^2E' - \tilde{X}\ ^2A_2'$

resolution : ~ 10 cm^{-1} (fwhm)
(monochromator settings)

$^{14}NO_3$

~~ν_3 (e')~~

a_1'

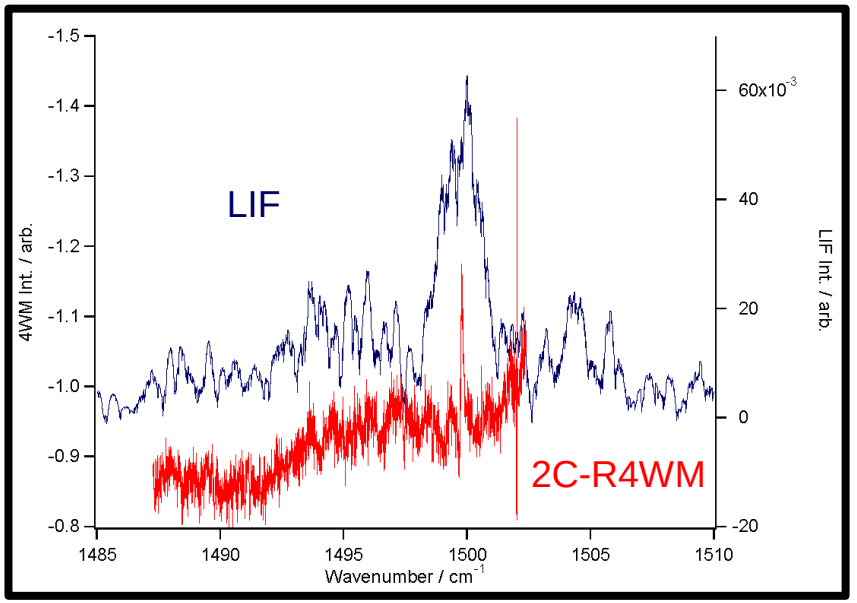

0 -500 -1000 -1500 -2000 -2500 -3000

Wavenumber / cm^{-1}

0+0 cm^{-1} band excitation

$\tilde{B}\ ^2E' - \tilde{X}\ ^2A_2'$

resolution : ~ 10 cm^{-1} (fwhm)
(monochromator settings)

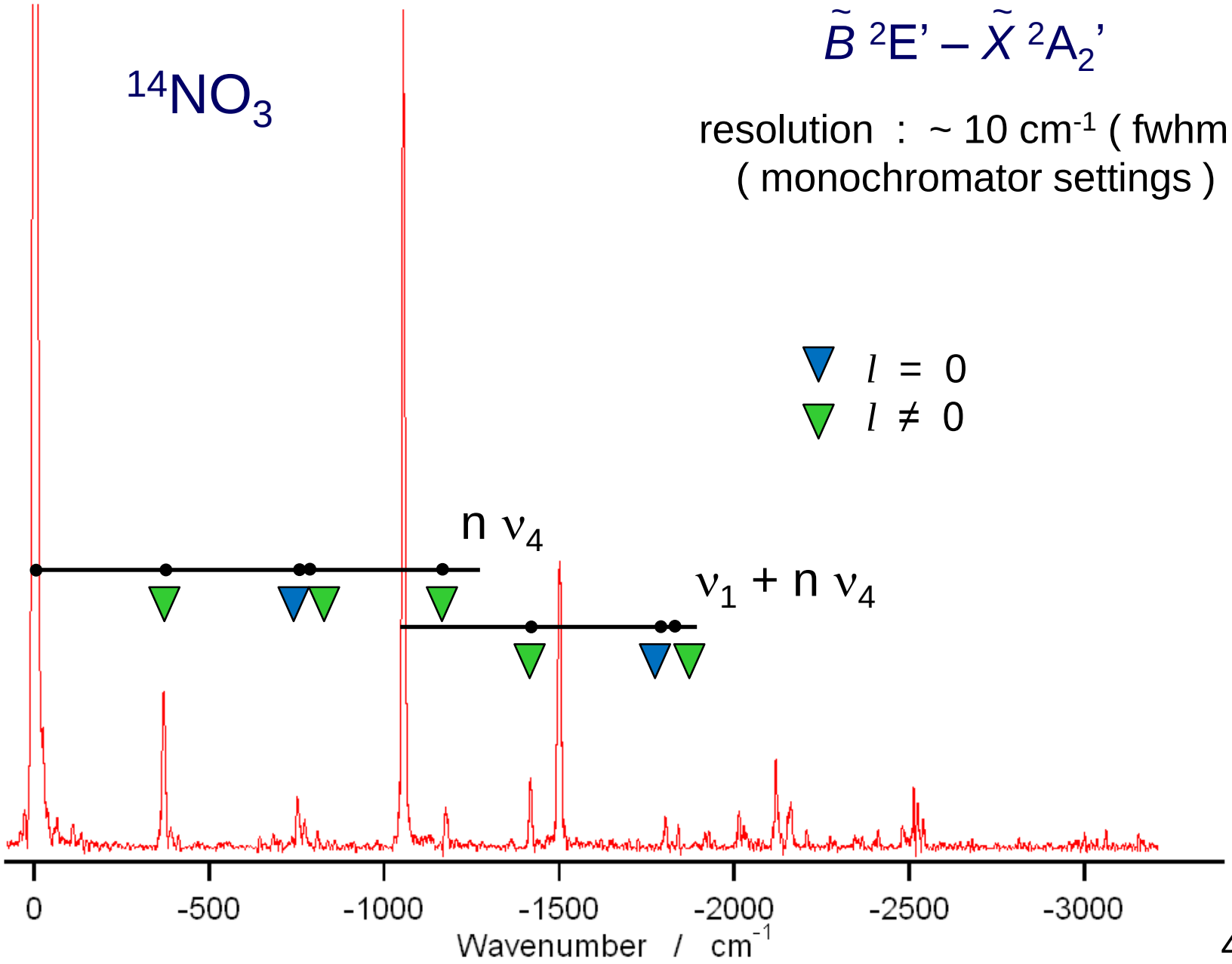

$^{14}NO_3$

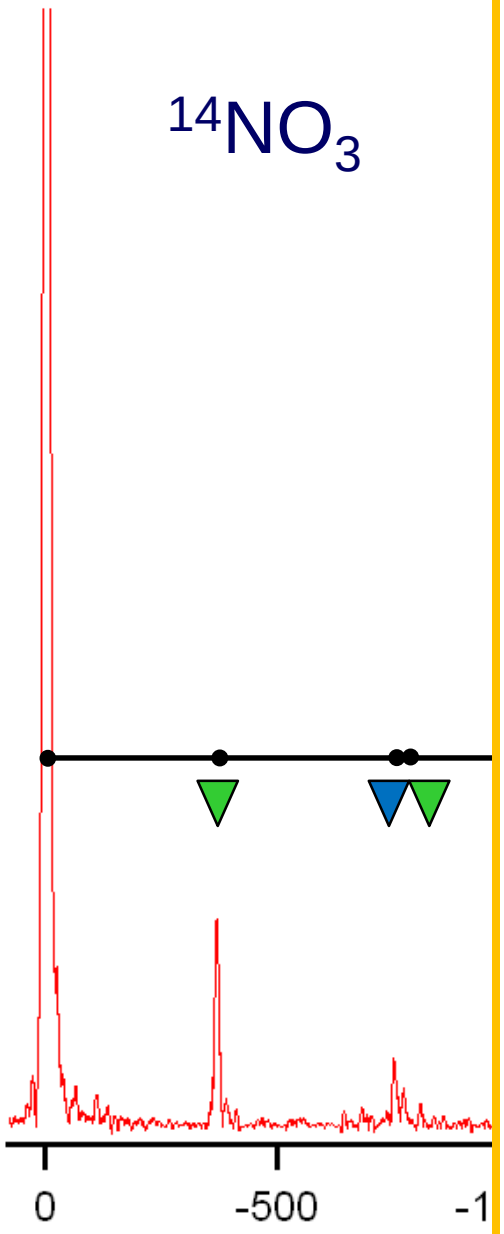
0
-500
-1

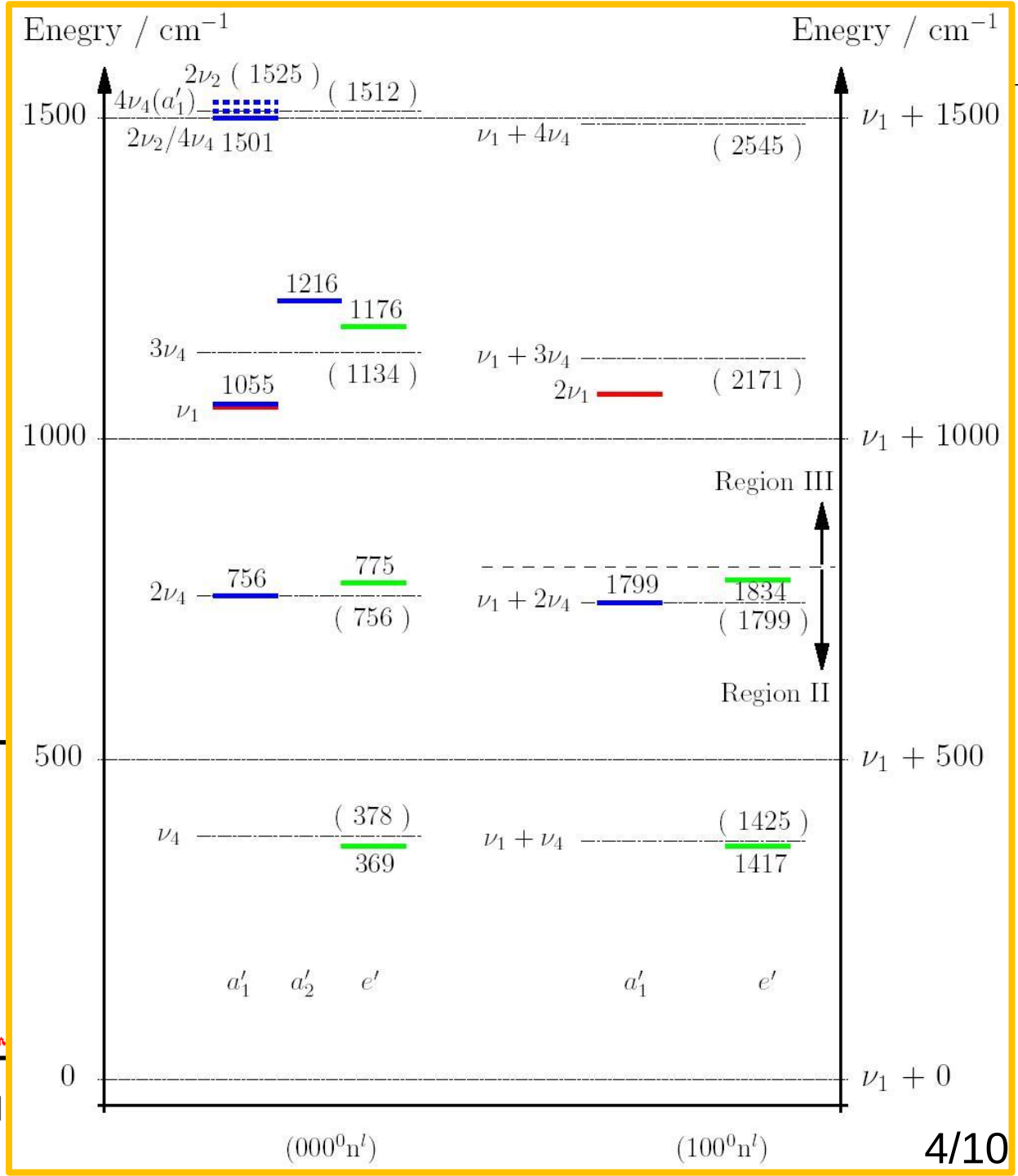
Energy / cm^{-1}
Energy / cm^{-1}
1500
1000
500
0
$2\nu_2$ (1525)
$4\nu_4(a_1')$
(1512)
$2\nu_2/4\nu_4$ 1501
$\nu_1 + 4\nu_4$
(2545)
$\nu_1 + 1500$
1216
1176
$3\nu_4$
(1134)
$\nu_1 + 3\nu_4$
$2\nu_1$
(2171)
1055
ν_1
$\nu_1 + 1000$
Region III
$2\nu_4$
756
775
(756)
$\nu_1 + 2\nu_4$
1799
1834
(1799)
Region II
$\nu_1 + 500$
ν_4
(378)
369
$\nu_1 + \nu_4$
(1425)
1417
a_1' a_2' e'
a_1' e'
$\nu_1 + 0$
(000^0n^l)
(100^0n^l)

0+0 cm^{-1} band excitation

$\tilde{B}\ ^2E' - \tilde{X}\ ^2A_2'$

resolution : ~ 10 cm^{-1} (fwhm)
(monochromator settings)

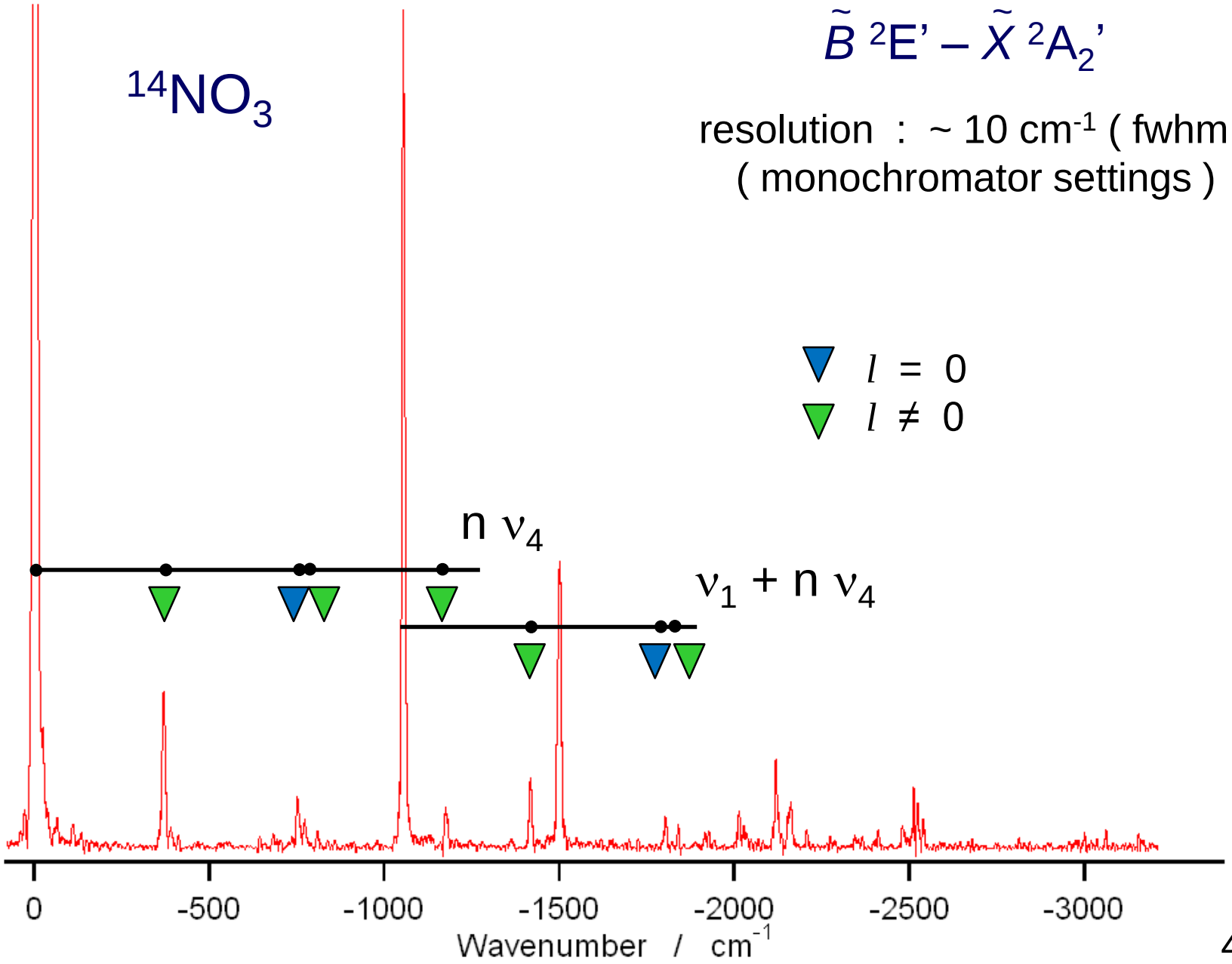

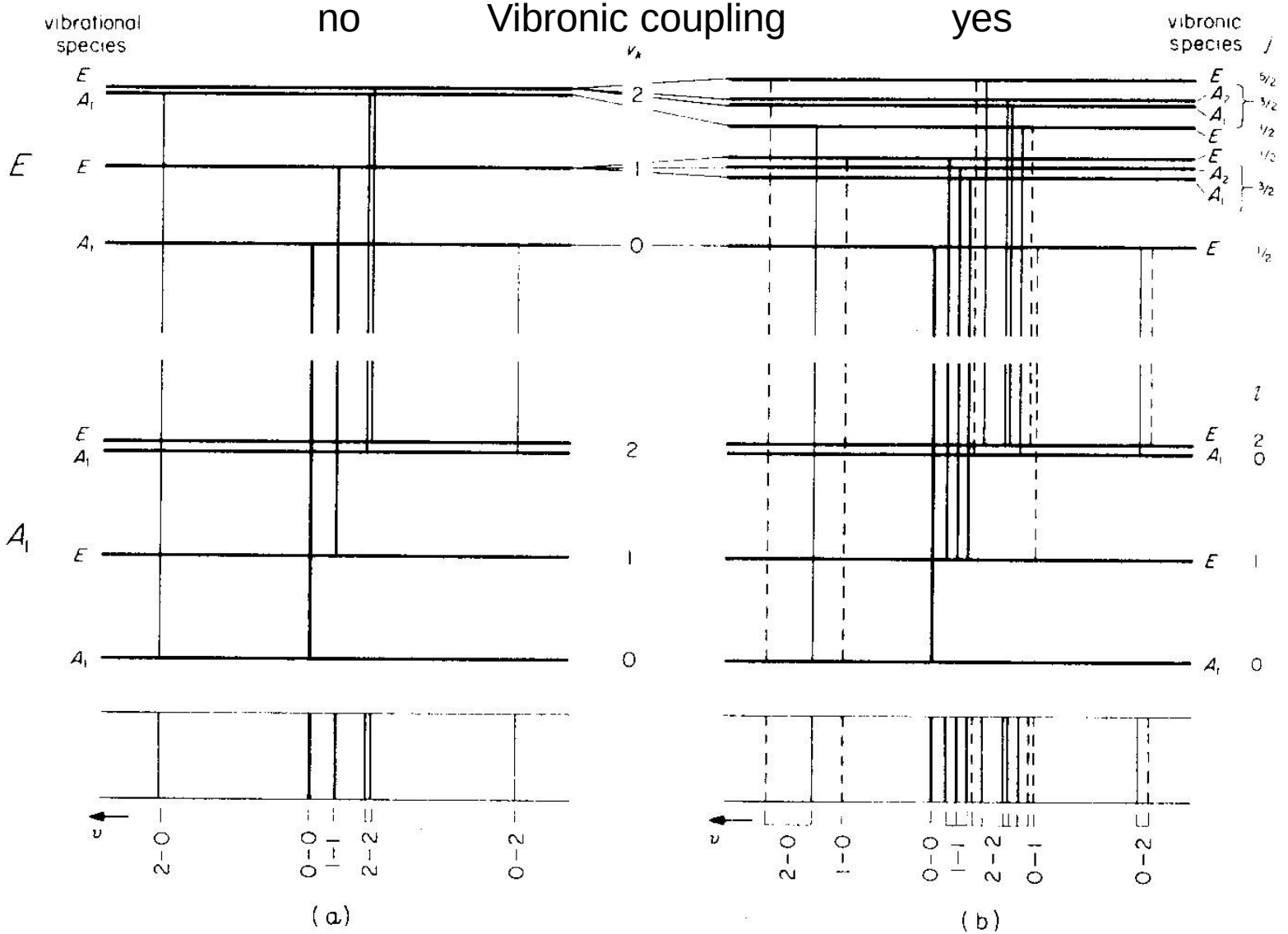

FIG. 61. **Vibrational transitions in a degenerate vibration ν_k for a $^1E - {}^1A_1$ electronic transition of a C_{3v} molecule** (*a*) **without and** (*b*) **with vibronic (Jahn–Teller) splitting.** Compare the caption of Fig. 59. The quantum number j at the right is well defined only if the three identical minima in the excited state can be combined into a trough of nearly cylindrical symmetry.

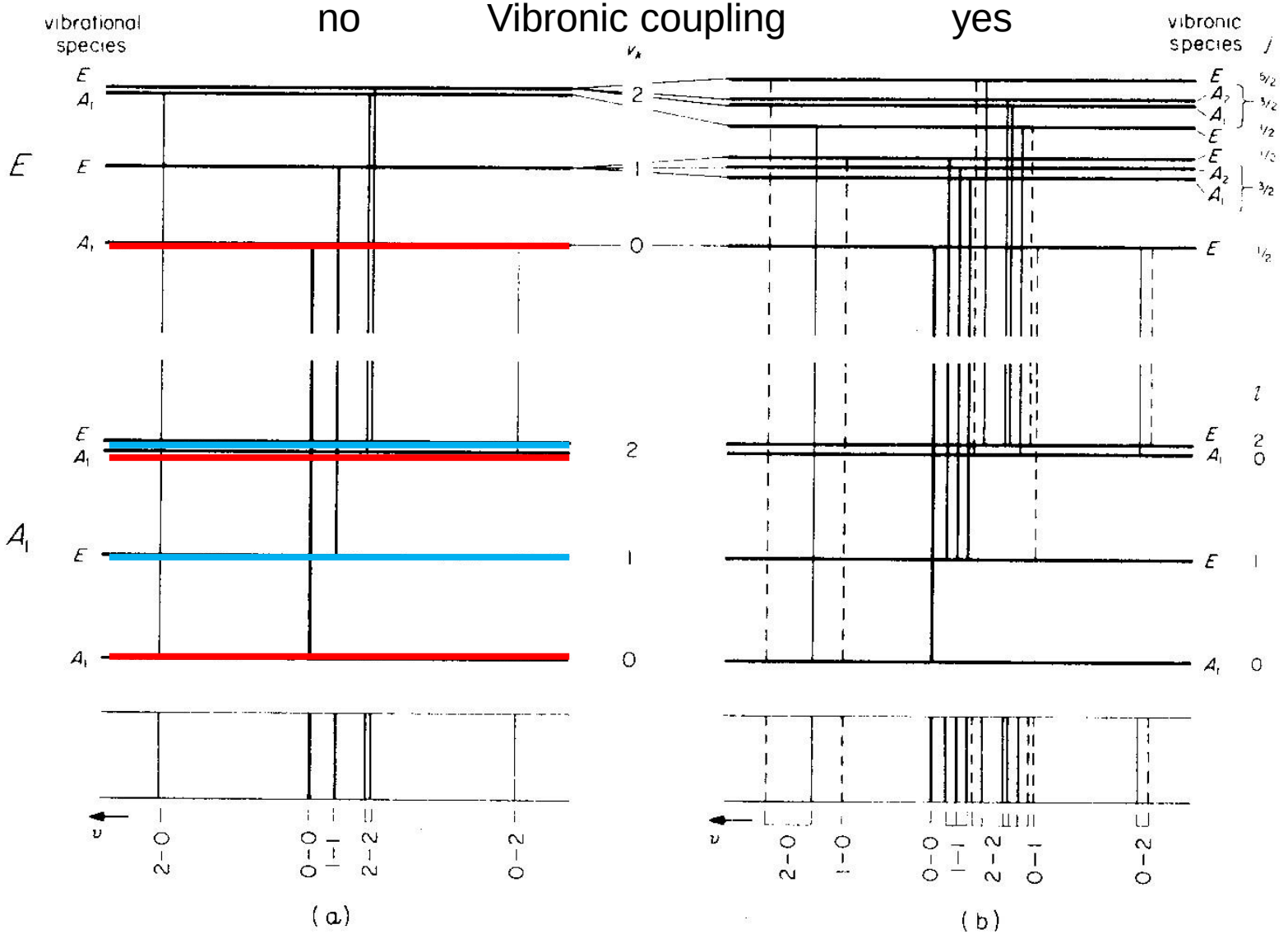

FIG. 61. **Vibrational transitions in a degenerate vibration ν_k for a $^1E - {}^1A_1$ electronic transition of a C_{3v} molecule** (*a*) **without and** (*b*) **with vibronic (Jahn–Teller) splitting.** Compare the caption of Fig. 59. The quantum number j at the right is well defined only if the three identical minima in the excited state can be combined into a trough of nearly cylindrical symmetry.

G. Herzberg, MM III.

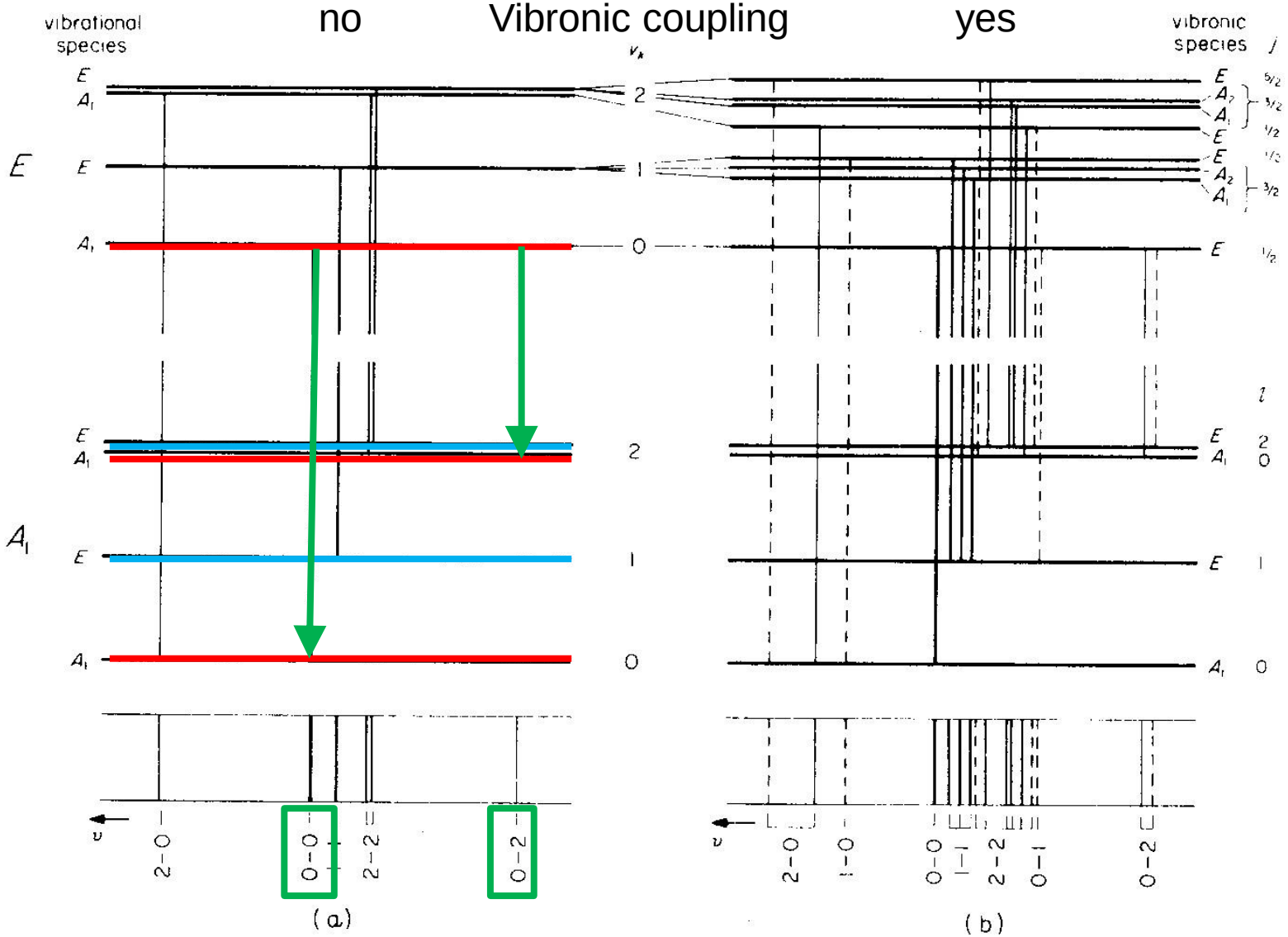

FIG. 61. **Vibrational transitions in a degenerate vibration ν_k for a $^1E - {}^1A_1$ electronic transition of a C_{3v} molecule** (*a*) **without and** (*b*) **with vibronic (Jahn–Teller) splitting.** Compare the caption of Fig. 59. The quantum number j at the right is well defined only if the three identical minima in the excited state can be combined into a trough of nearly cylindrical symmetry.

G. Herzberg, MM III.

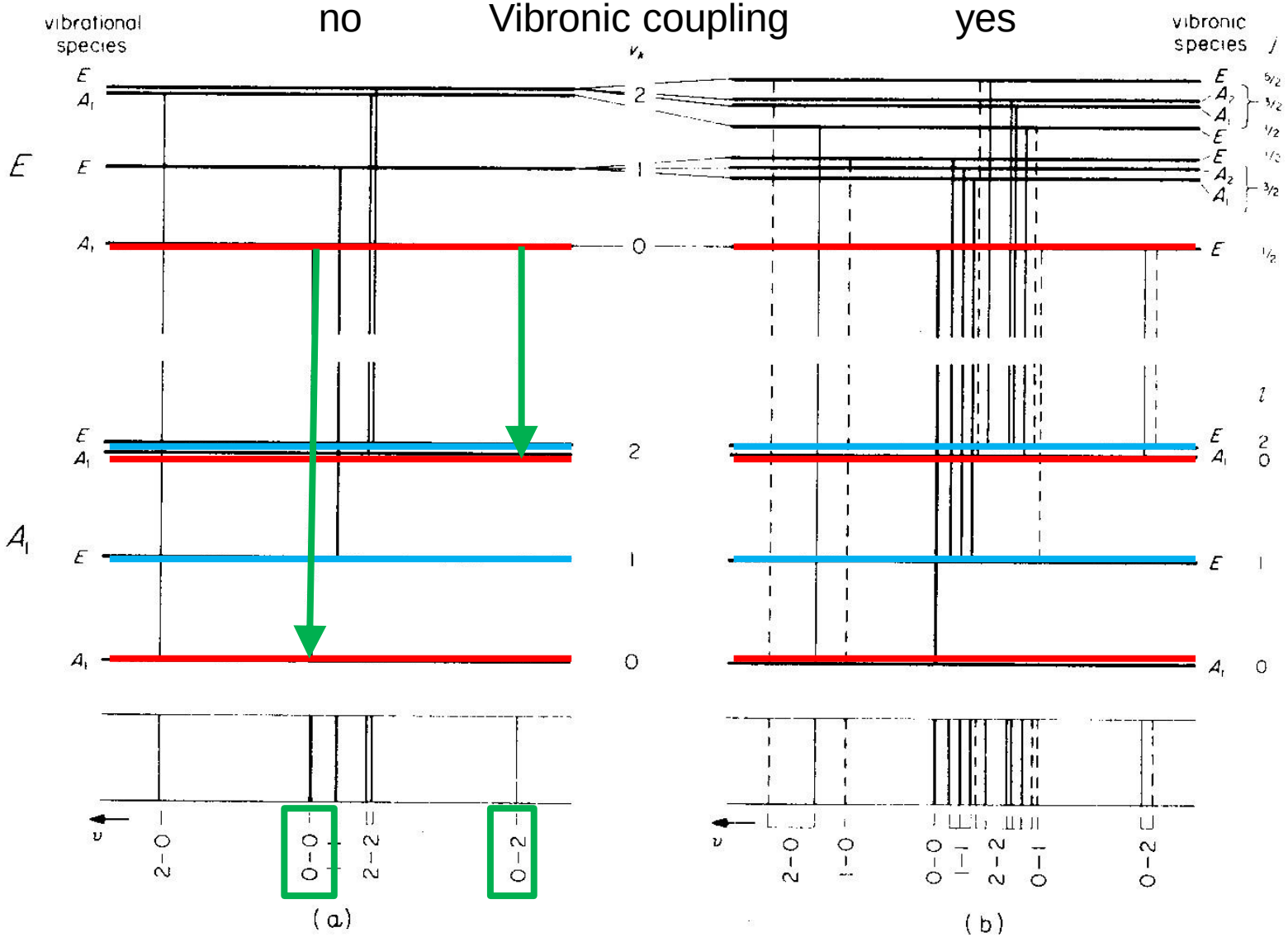

FIG. 61. **Vibrational transitions in a degenerate vibration ν_k for a $^1E - {}^1A_1$ electronic transition of a C_{3v} molecule** (*a*) **without and** (*b*) **with vibronic (Jahn–Teller) splitting.** Compare the caption of Fig. 59. The quantum number *j* at the right is well defined only if the three identical minima in the excited state can be combined into a trough of nearly cylindrical symmetry.

G. Herzberg, MM III.

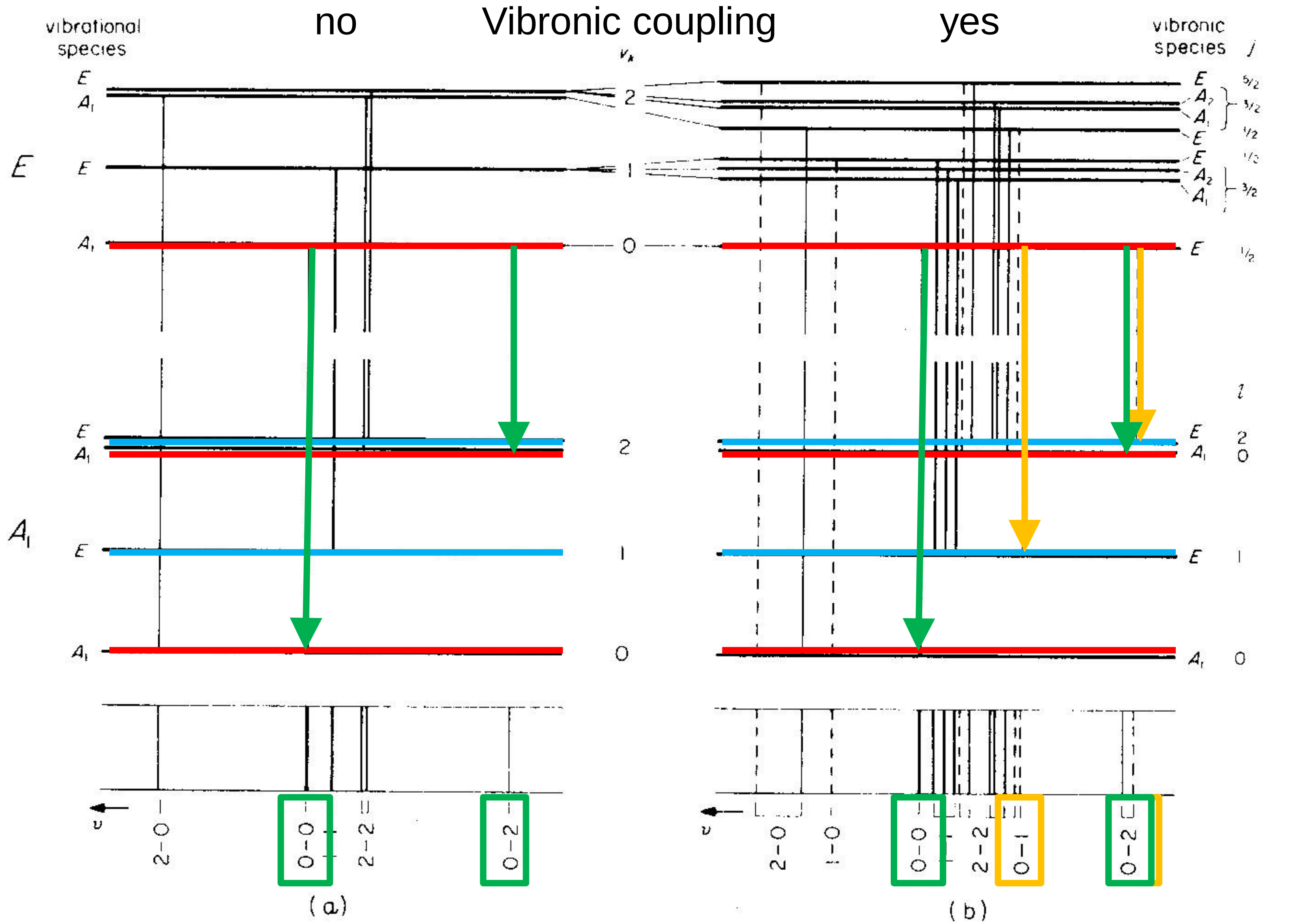

FIG. 61. **Vibrational transitions in a degenerate vibration ν_k for a $^1E - {^1A_1}$ electronic transition of a C_{3v} molecule (a) without and (b) with vibronic (Jahn–Teller) splitting.** Compare the caption of Fig. 59. The quantum number j at the right is well defined only if the three identical minima in the excited state can be combined into a trough of nearly cylindrical symmetry.

G. Herzberg, MM III.

Dispersed fluorescence spectra

$^{14}NO_3$

resolution : fwhm 7 cm^{-1}
peak accuracy : ±2 cm^{-1}

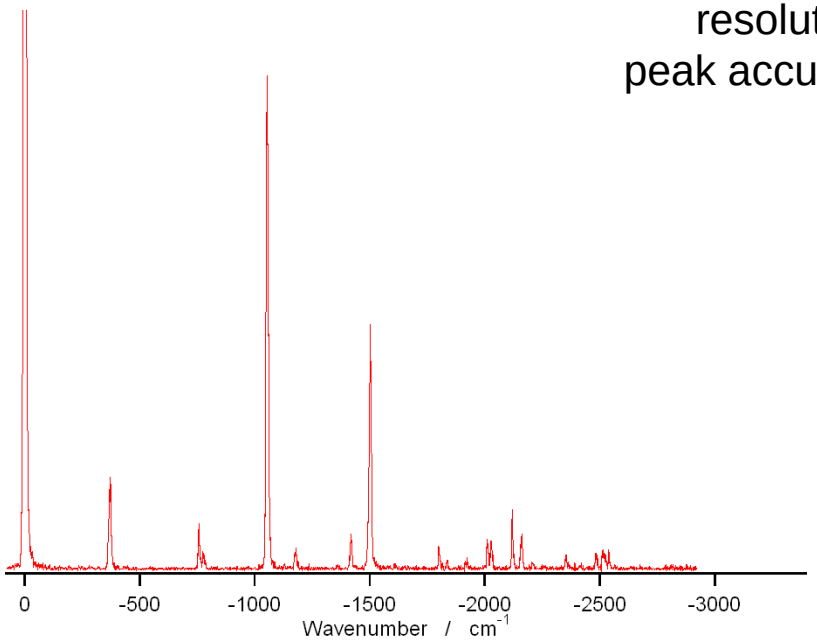

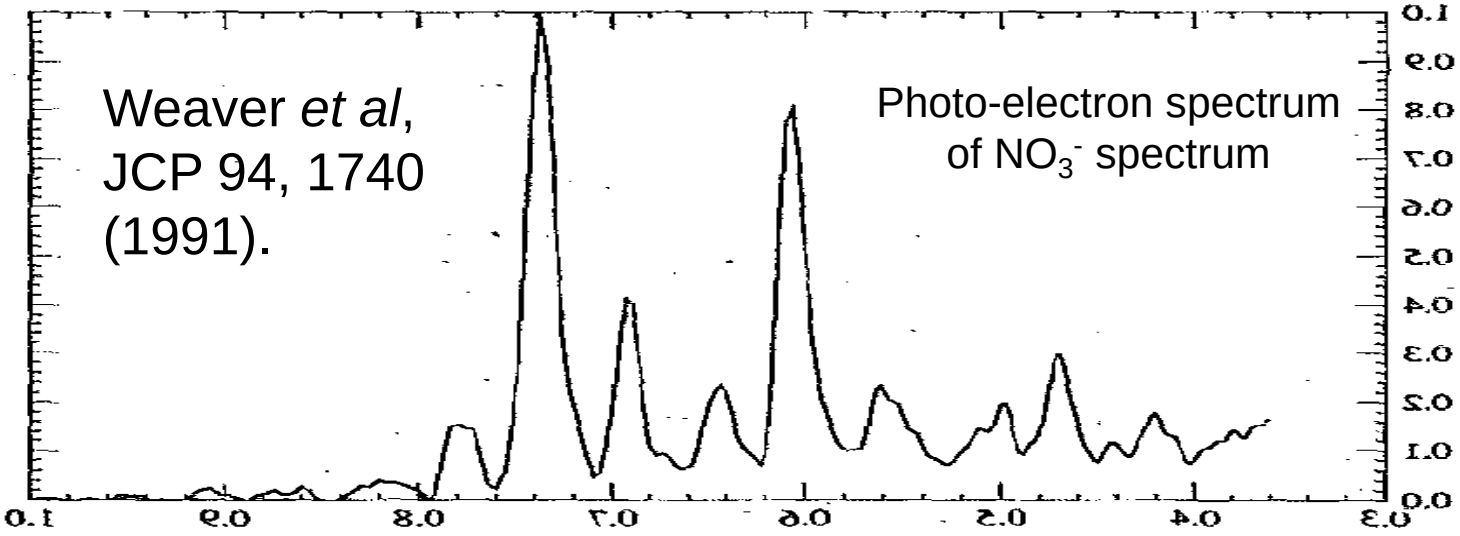

Dispersed fluorescence spectra

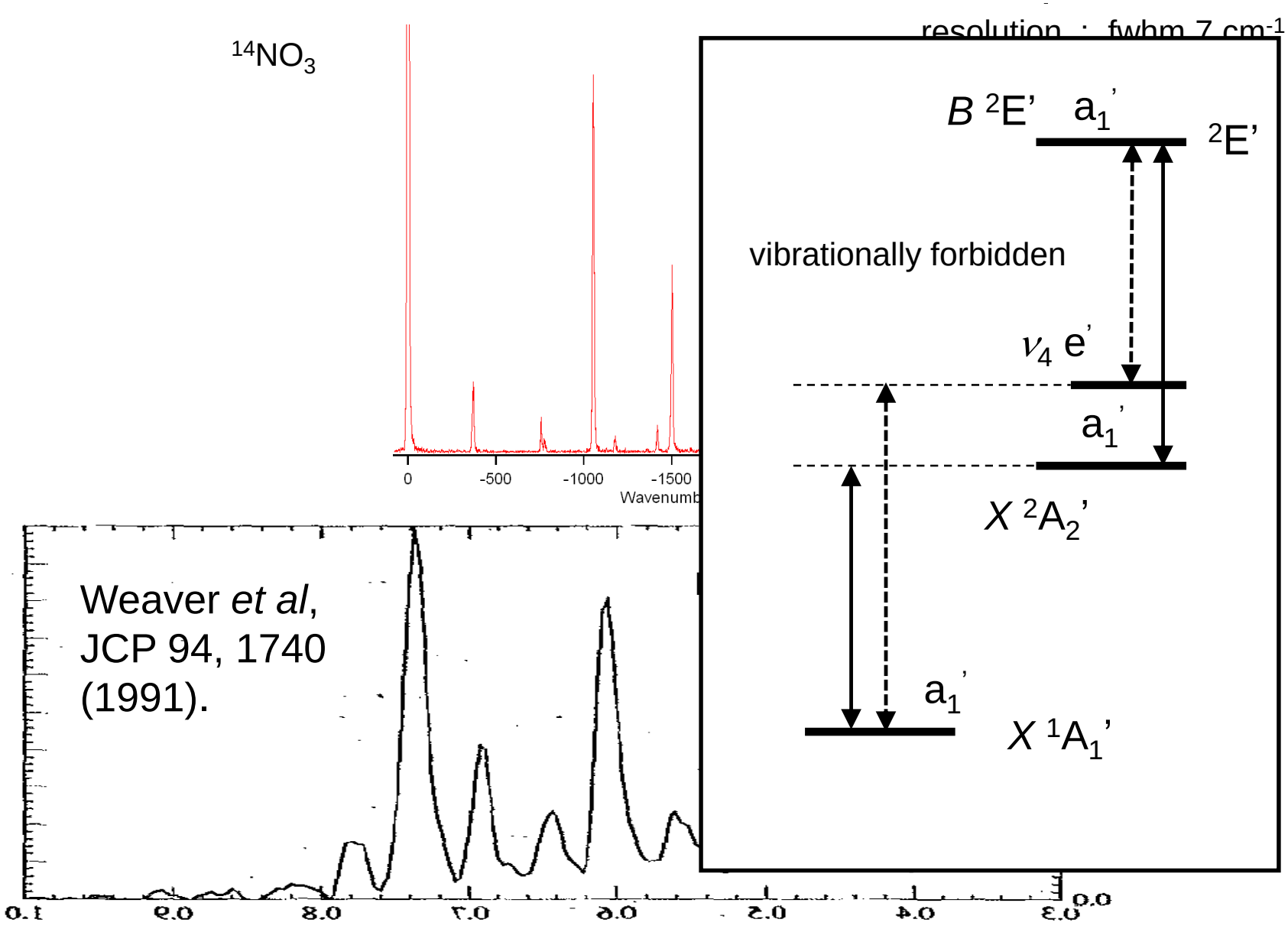

Dispersed fluorescence spectra

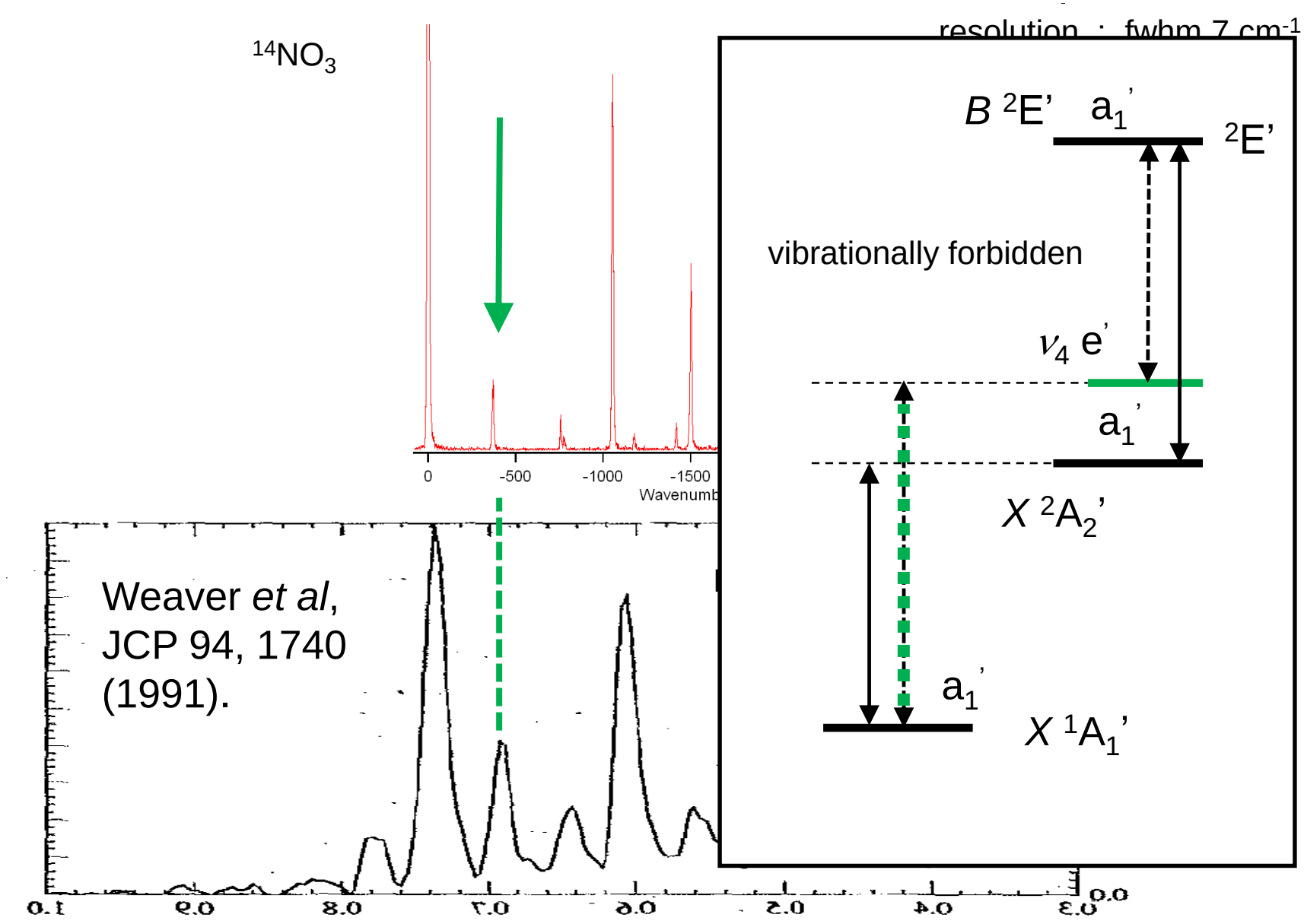

Dispersed fluorescence spectra

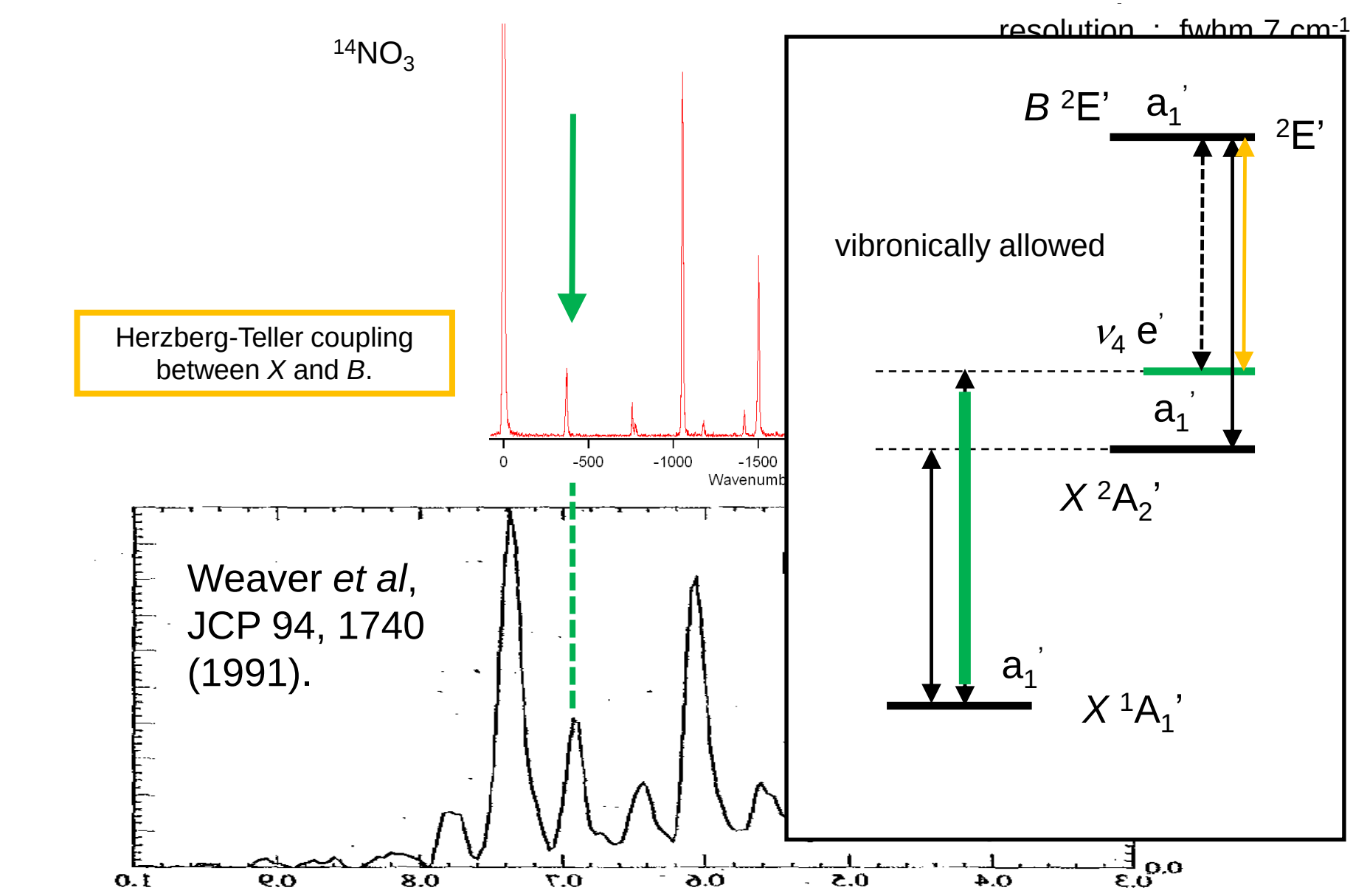

Dispersed fluorescence spectra

$^{14}NO_3$

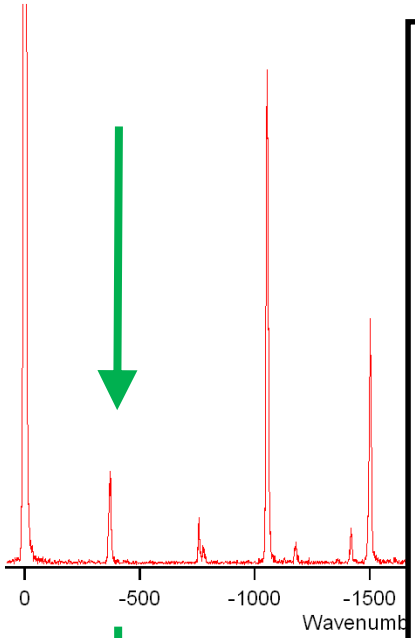

resolution : fwhm 7 cm^{-1}

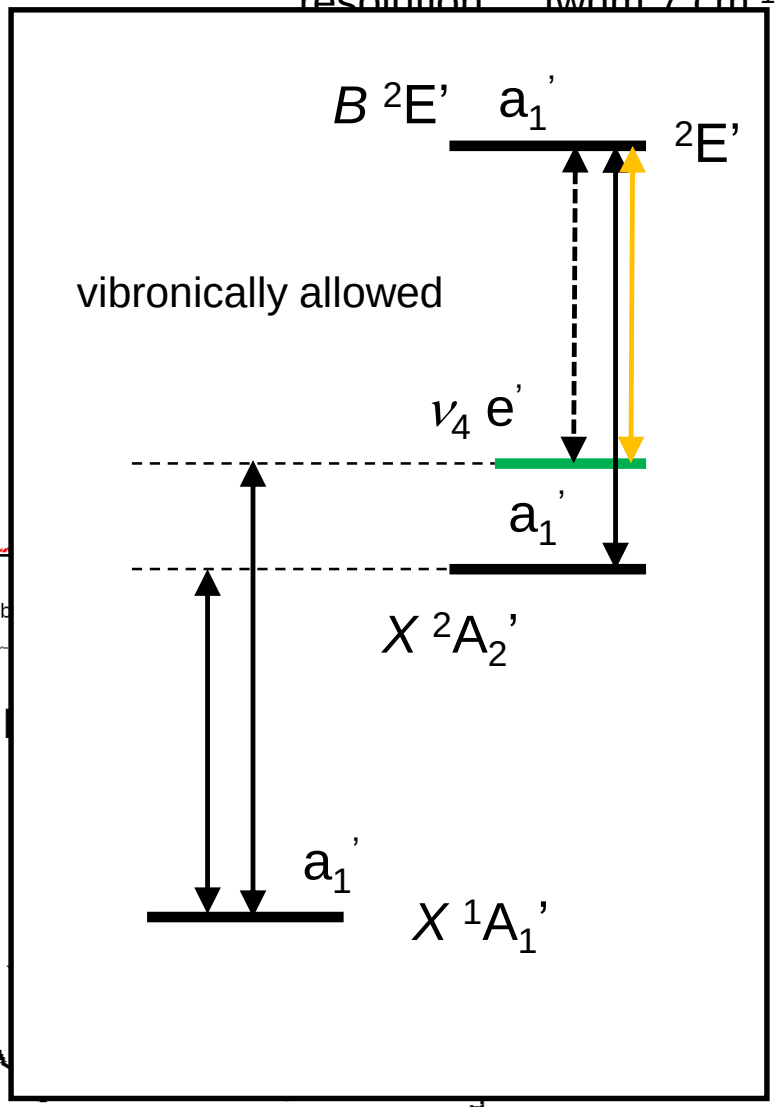

Herzberg-Teller coupling between *X* and *B*.
But the strength is too large to maintain D_{3h} in *X*.

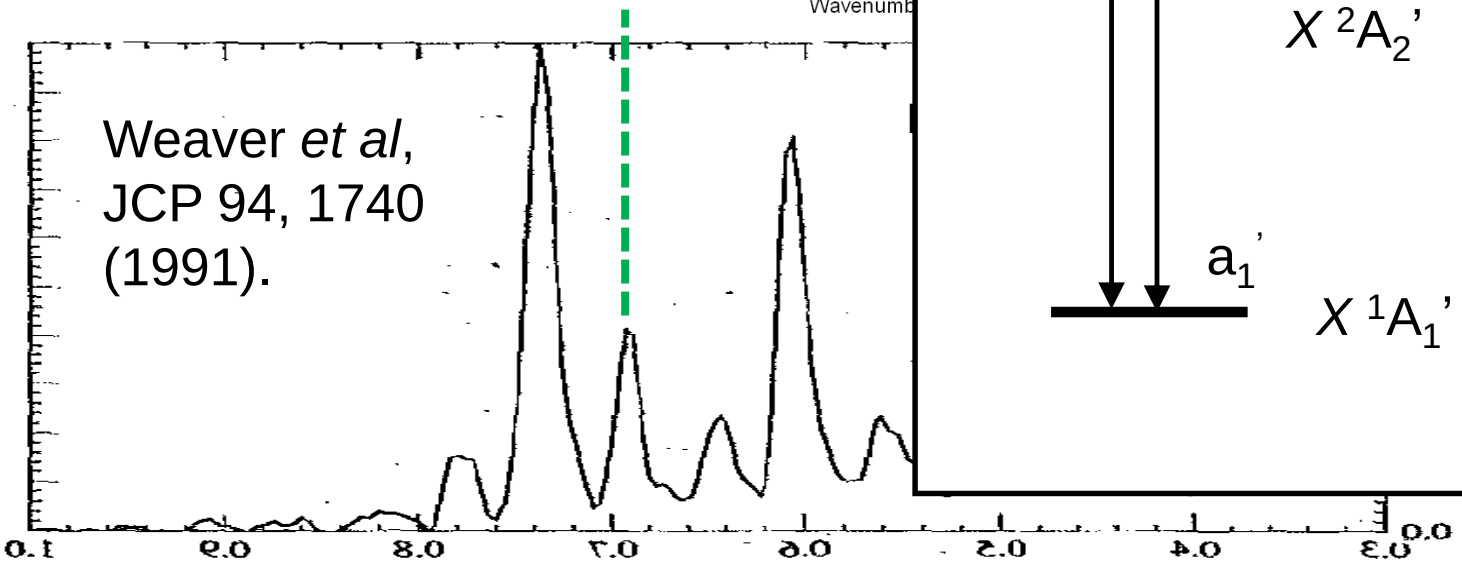

Weaver *et al*, JCP 94, 1740 (1991).

Dispersed fluorescence spectra

$^{14}NO_3$

Herzberg-Teller coupling between *X* and *B*.
But the strength is too large to maintain D_{3h} in *X*.

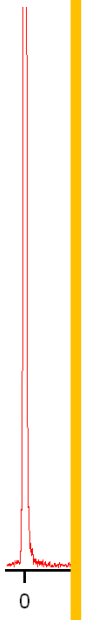

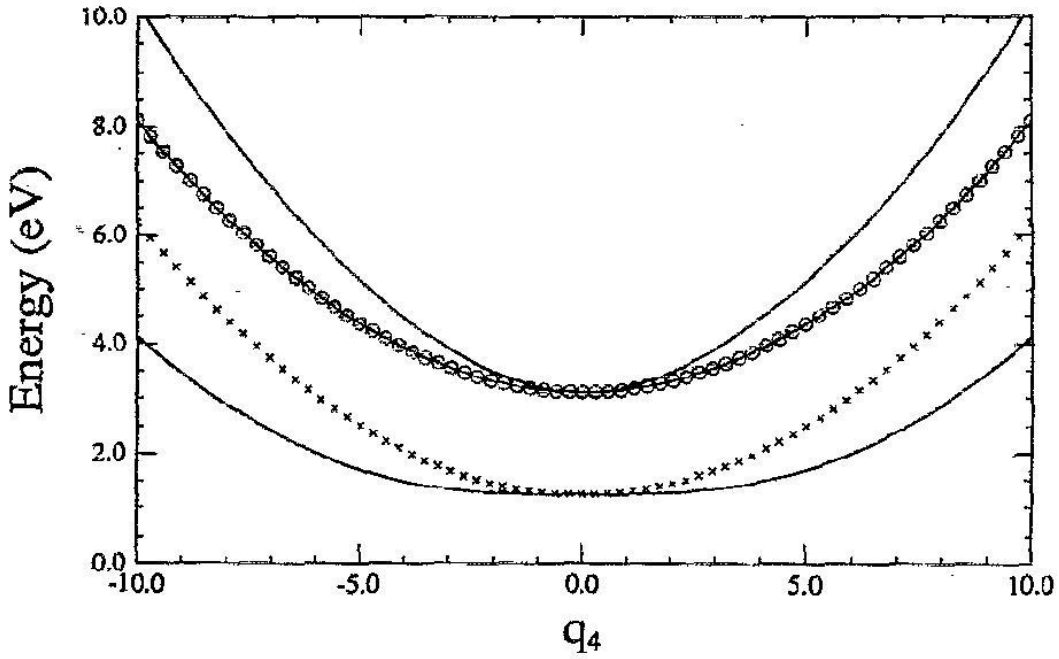

FIG. 8. Potential energy of the NO_3 $^2A_2'$ and $^2E'$ states as a function of q_4, the dimensionless normal coordinate. The solid curves are the adiabatic pseudo-Jahn–Teller-perturbed potentials calculated from Eq. (15), with $\omega_4 = 0.1$ eV (805 cm^{-1}) and $\lambda_4 = 0.290$ eV. We have neglected Jahn–Teller coupling in the $^2E'$ state. The unperturbed harmonic oscillator potentials for the $^2A_2'$ (×) and $^2E'$ (○) states are also shown.

Weaver *et al*, JCP 94, 1740 (1991).

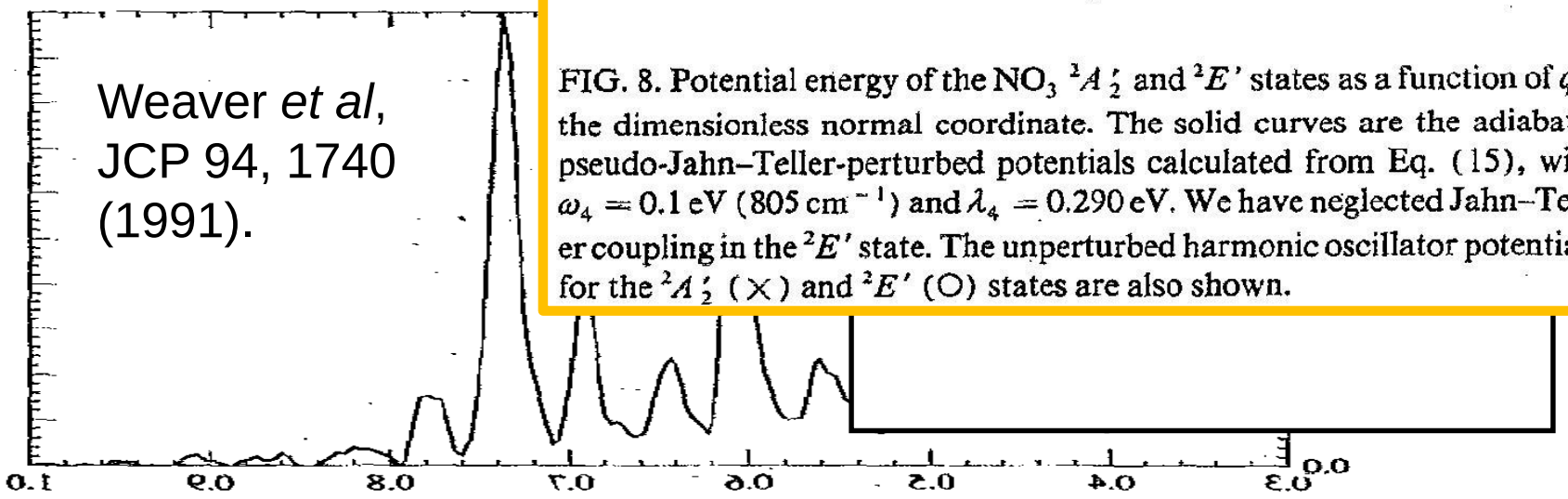

Dispersed fluorescence spectra

$^{14}NO_3$

resolution : fwhm 7 cm^{-1}
peak accuracy : ±2 cm^{-1}

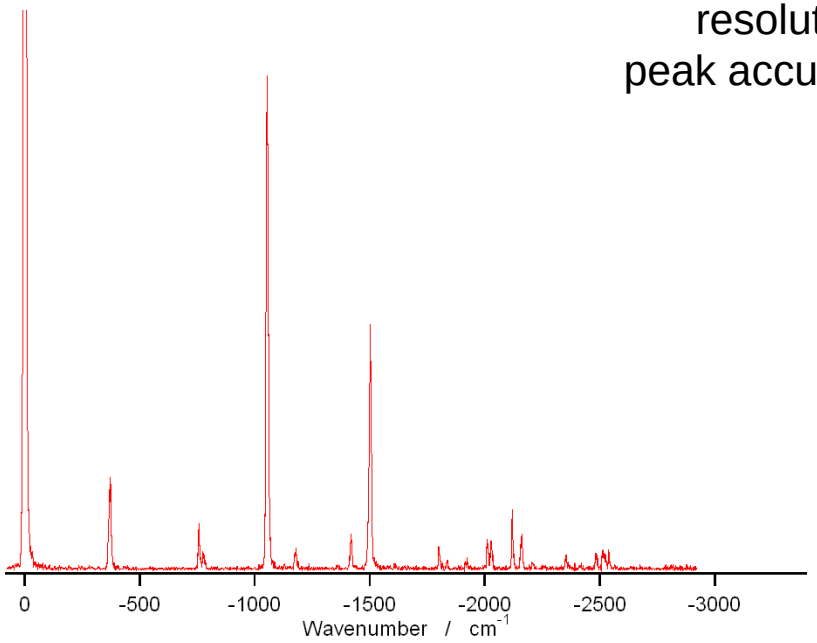

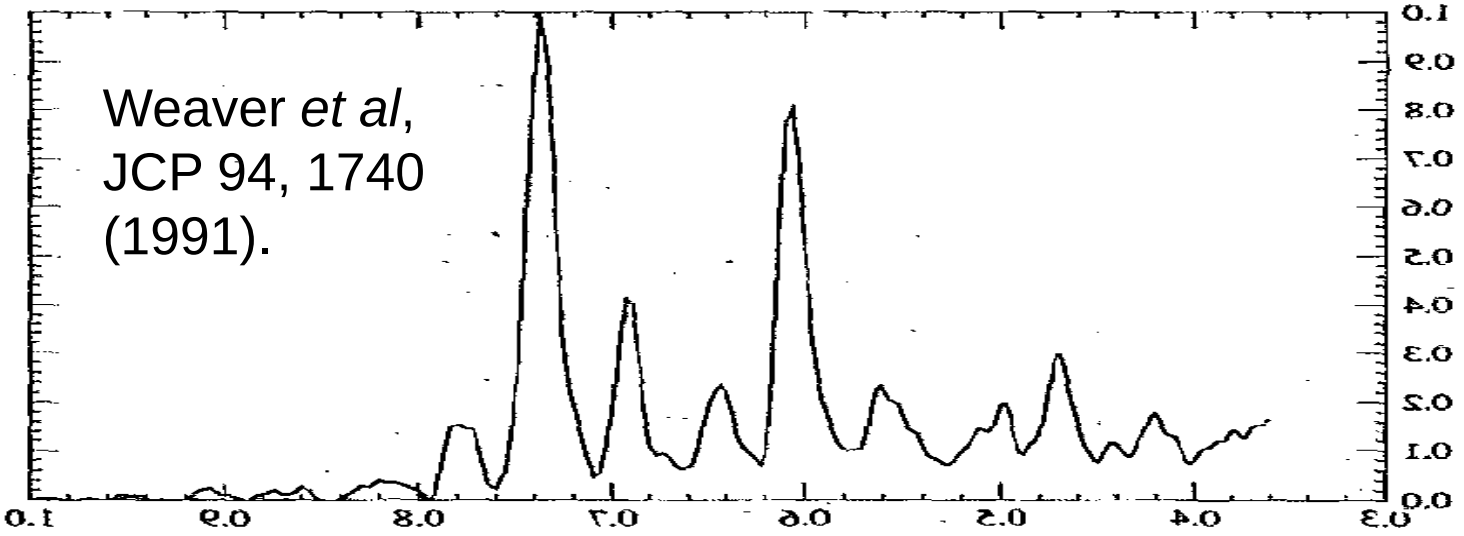

l is not a good quantum number, but K is
(at degenerated vibrational mode).

$$|K;\ \Lambda;\ v_4, l\rangle \neq |\Lambda\rangle |v_4, l\rangle$$ (Vibronic coupling)

where $K = \Lambda + l$

Λ : projection of electronic orbital angular momentum

l : projection of vibrational angular momentum

l is not a good quantum number, but K is
(at degenerated vibrational mode).

$$|K;\ \Lambda;\ v_4, l\rangle \neq |\Lambda\rangle |v_4, l\rangle$$ (Vibronic coupling)

where $K = \Lambda + l$

Λ : projection of electronic orbital angular momentum

l : projection of vibrational angular momentum

At the $\tilde{X}\ ^2A_2'$, $\tilde{A}\ ^2E''$, and $\tilde{B}\ ^2E'$ states, unpaired electron is localized on O's, and has no contribution to any chemical bonds. It is easily expected that the degenerate vibration can induce motion of the electron.

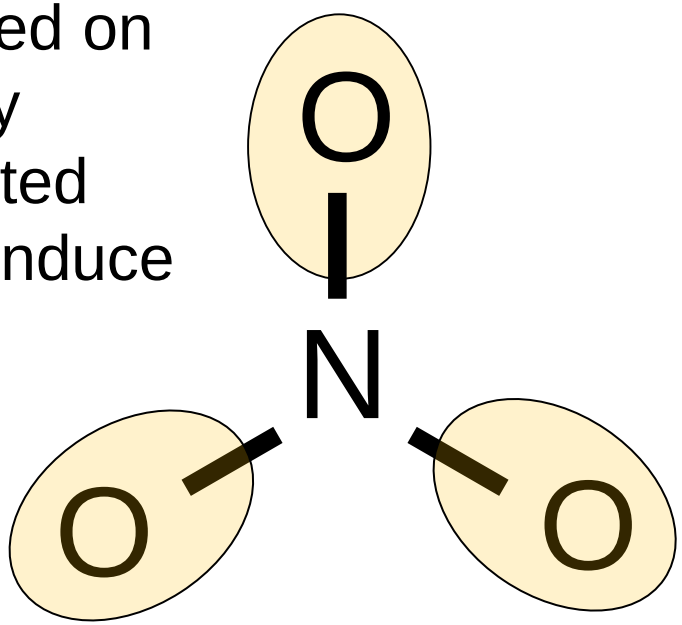

$2p_x$

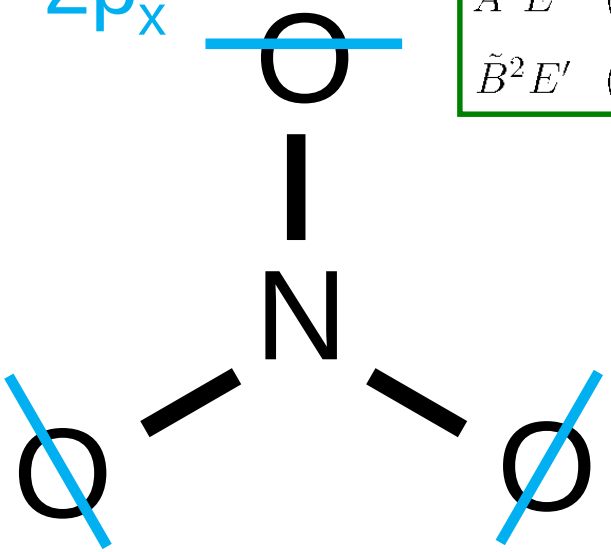

D_{3h}

$\tilde{X}^2A_2'$	(core)	$\underbrace{(4a_1')^2(3e')^4}_{\sigma}$	$\underbrace{(1a_2'')^2}_{\pi}$	$\underbrace{(1e'')^4(4e')^4(1a_2')^1}_{\pi}$	$\underbrace{(2a_2'')^0}_{\pi^*}$	$\underbrace{(5a_1')^0(5e')^0}_{\sigma^*}$
$\tilde{A}^2E''$	(core)	$(4a_1')^2(3e')^4$	$(1a_2'')^2$	$(1e'')^3(4e')^4(1a_2')^2$	$(2a_2'')^0$	$(5a_1')^0(5e')^0$
$\tilde{B}^2E'$	(core)	$(4a_1')^2(3e')^4$	$(1a_2'')^2$	$(1e'')^4(4e')^3(1a_2')^2$	$(2a_2'')^0$	$(5a_1')^0(5e')^0$

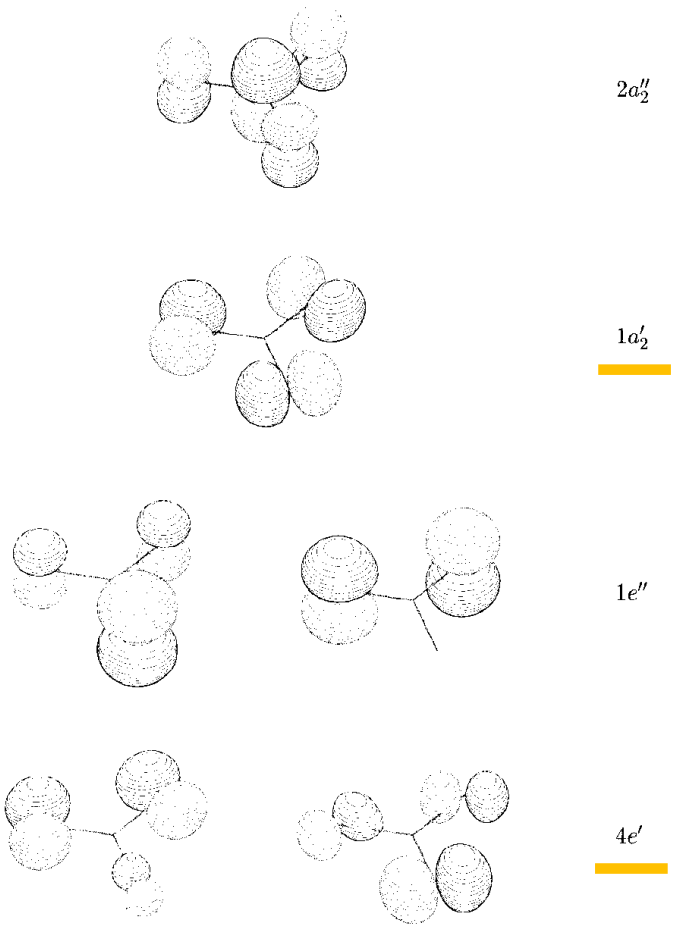

Eisfeld and Morokuma, J. Chem. Phys. 114, 9430 (2001).

FIG. 1. Selected molecular orbitals of NO_3 as calculated by CASSCF at D_{3h} geometry with a N–O distance of 1.240 Å.

l is not a good quantum number, but K is
(at degenerated vibrational mode).

$$|K;\ \Lambda;\ v_4, l\rangle \neq |\Lambda\rangle |v_4, l\rangle$$ (Vibronic coupling)

where $K = \Lambda + l$

Λ : projection of electronic orbital angular momentum

l : projection of vibrational angular momentum

At the $\tilde{X}\ ^2A_2'$, $\tilde{A}\ ^2E''$, and $\tilde{B}\ ^2E'$ states, unpaired electron is localized on O's, and has no contribution to any chemical bonds. It is easily expected that the degenerate vibration can induce motion of the electron.

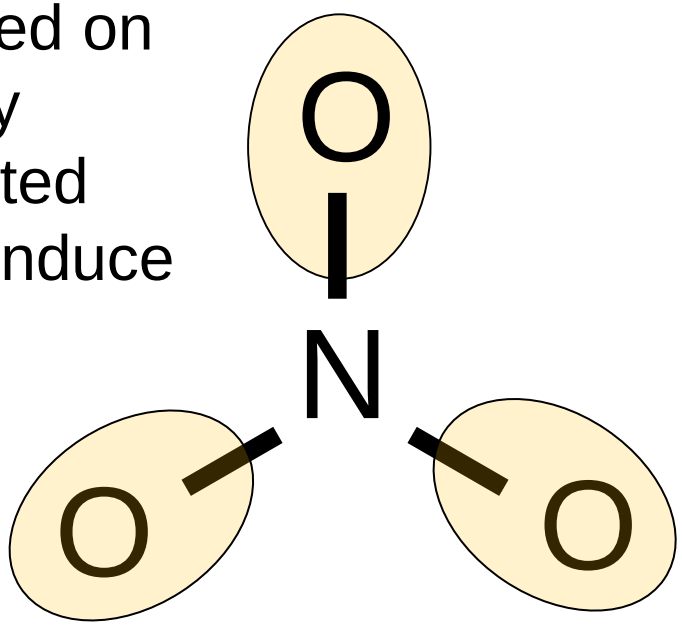

l is not a good quantum number, but K is.

$$|K;\ \Lambda;\ v_4, l\rangle \neq |\Lambda\rangle |v_4, l\rangle$$

where $K = \Lambda + l$

Λ : projection of electronic orbital angular momentum

l : projection of vibrational angular momentum

Conclusions

To understand the ν_4 progressions with regular intensity distribution, we proposed our interpretation, i.e.

even in the $\tilde{X}\ ^2A_2'$ state,

vibronic coupling is induced

at the non-degenerate vibrational mode

(can be called as degenerate vibrationally induced vibronic coupling).

We have the other important observations:

(1) large splitting of the $3\nu_4$ (a_1') and (a_2') levels (observed by LIF),

(2) large spin splitting at the $3\nu_4$ (a_1') level (observed by 2C-R4M).

Conclusions

To understand the ν_4 progressions with regular intensity distribution, we proposed our interpretation, i.e.

even in the $\tilde{X}\ ^2A_2'$ state,

vibronic coupling is induced

at the non-degenerate vibrational mode

(can be called as degenerate vibrationally induced vibronic coupling).